

# Majority-vote on directed Erdős–Rényi random graphs

F.W.S. Lima

*Departamento de Física, Universidade Federal do Piauí  
Teresina - PI, 64049-550, Brazil*

A.O. Sousa

*Departamento de Física Teórica e Experimental, Universidade Federal do Rio  
Grande do Norte  
Natal-RN, 59072-970, Brazil*

M.A. Sumuor

*Physics Department, Al-Aqsa University  
Gaza, Gaza Strip, P. O. Box 4051, Pallestian Authority*

---

## Abstract

Through Monte Carlo Simulation, the well-known majority-vote model has been studied with noise on *directed* random graphs. In order to characterize completely the observed order-disorder phase transition, the critical noise parameter  $q_c$ , as well as the critical exponents  $\beta/\nu$ ,  $\gamma/\nu$  and  $1/\nu$  have been calculated as a function of the connectivity  $z$  of the random graph.

*Key words:* Networks, Majority-vote model

*PACS:* 64.60.Cn, 05.10.Ln, 64.60.Fr, 75.10.Hk

---

## 1 Introduction

The majority-vote model (MVM) [1,2], a nonequilibrium model defined by stochastic dynamics with local rules and with up-down symmetry, defined on

---

*Email addresses:* `wel@ufpi.br` (F.W.S. Lima), `aosousa@dfte.ufrn.br` (A.O. Sousa), `msumoor@alagsa.edu.ps` (M.A. Sumuor).

regular lattices shows a second-order phase transition with critical exponents  $\beta, \gamma, \nu$  – which characterize the system in the vicinity of the phase transition – identical [2,3,4] with those of equilibrium Ising model [5,6]. More general, it has been argued that the existence of up-down symmetry in two-state dynamic systems implies the same critical behavior (same universality class) of the equilibrium Ising model [7,3,8].

On the other hand, MVM on the complex networks exhibit different behavior, i.e., it belongs to different universality class [9,10,11,12]. Campos *et al.* investigated MVM on a small-world network [9], which was constructed using the square lattice (SL) by the rewiring procedure [13]. Campos *et al.* found that the critical exponents  $\gamma/\nu$  and  $\beta/\nu$  are different from these of the Ising model [6] and depend on the rewiring probability. Pereira *et al.* [12] studied MVM on Erdős–Rényi’s (ER) classical random graphs [14,15], and Lima *et al.* [10] also studied this model on random Voronoy–Delaunay [16] lattice with periodic boundary conditions. Very recently Lima [11] studied the MVM on directed Albert–Barabási (AB) network [17] and contrary to the Ising model [5] on these networks [18], the order/disorder phase transition is observed in this system. The calculated  $\beta/\nu$  and  $\gamma/\nu$  exponents are different from those for the Ising model [6] and depend on the value of connectivity  $z$  of AB network. The latter was observed also for *undirected* ER random graph [12].

In this paper we study the Majority-vote model with noise on *directed* Erdős–Rényi (ER) random graphs [14,15]. Through Monte Carlo (MC) simulations and standard finite-size scaling techniques we determine the critical exponents for several values of the connectivity  $z$  of the graph, in order to characterize the observed order-disorder phase transition.

## 2 The Model

The majority-vote model, on *directed* Erdős–Rényi (ER) random graphs, is defined [2,10,12,14,15,19] by a set of ”voters” or spins variables  $\sigma_i = \pm 1$ , located on every site (or node) of a *directed* ER graph. The system dynamics is as follows: For each spin we determine the sign of the majority of its neighboring spins. With probability  $q$ , known as the noise parameter, the spin takes the opposite sign of the majority of its neighbors, otherwise it takes the same sign. It is important to emphasize that the noise parameter  $q$  plays the role of the temperature in equilibrium systems and measures the probability of aligning anti-parallel to the majority of neighbors. The probability  $w_i$  of a single spin

flip is given by

$$w(\sigma_i) = \frac{1}{2} \left[ 1 - (1 - 2q) \sigma_i S \left( \sum_{\delta=1}^{k_i} \sigma_{i+\delta} \right) \right], \text{ with } S(x) = \begin{cases} \frac{x}{|x|}, & \text{se } x \neq 0 \\ 0, & \text{se } x = 0 \end{cases} \quad (1)$$

where the summation is over all  $k_i$  sites connected to spin  $\sigma_i$ . It is worth to mention that this probability exhibits up-down symmetry, i.e.,  $w(\sigma_i) = w(-\sigma_i)$  under the change of the spins in the neighborhood of  $\sigma_i$ .

It is argued [1] that on a square lattice there exists two phases for sufficiently small  $q$ , with a formation of an island of up spins on a sea of down spins. The size of this island follows a birth-and-death process in which the death rate is larger than the birth rate, thus preventing the growth of the island and keeping the down spin phase stable. By symmetry, there must exist another phase with spins up. However, if the up-down symmetry of the spin flip probability is broken, no phase transition is expected, as in the Ising model [1]. In two dimensions this model has a ferromagnetic stationary phase for  $0 < q < q_c$  undergoing a second-order phase transition to a paramagnetic phase at  $q_c$  ( $q_c = 0.075$  for a square lattice). The static critical behavior is Onsager-like [2,3,8], and according to the argument of Grinstein *et al.* [7], its dynamic critical behavior is the same as model Ising.

Indeed, the majority-vote is a particular case of a general class of polling models [20,21] composed by interacting two-state opinion agents. The main result of the most opinion formation models is that the dynamical rule leads to an opinion polarization of the whole population along one of the two competing opinions [20,21,22]. Recently, the contrarian concept - agents which have the opinion opposite to that of the majority - was introduced to take into account some peculiar behavior of the agents [23]. With a small fraction of contrarians, the system no longer leads to total polarization: the minority opinion does not disappear from the population. Above a critical fraction of contrarians, polarization does not occur, and the two possible opinions are shared each by half the agents [23,24].

Depending on the nature of the interactions, networks can be directed or undirected [25]. In directed networks, the interaction between any two nodes has a well-defined direction, which represents, for example, the direction of material flow from a substrate to a product in a metabolic reaction, or the direction of information flow from a transcription factor to the gene that it regulates. In undirected networks, the links do not have an assigned direction. For example, in protein interaction networks a link represents a mutual binding relationship: if protein A binds to protein B, then protein B also binds to protein A. In other words, in undirected networks, if a node  $A$  is linked to  $B$ , then  $B$  must also be linked to  $A$ , while in directed ones, if a node  $A$  is linked

to  $B$ ,  $B$  may not be linked to  $A$ , but to some node else instead. In the present work, we only consider directed graphs.

Starting with  $N$  disconnected nodes, the Erdős–Rényi network are generated by connecting couples of randomly selected nodes with a probability  $0 < p < 1$  for every pair, prohibiting multiple connections (i.e., couples of nodes connected by more than one link), until the number of edges equals  $z$  (connectivity or number of links of a node). In the limit  $N \rightarrow \infty$ , it is found that the tail (high  $z$  region) of the degree distribution  $P(z)$  decreases exponentially, which indicates that nodes that significantly deviate from the average are extremely rare. The clustering coefficient - which is the probability that two neighbors of the same node are also mutual neighbors [13,26] - is independent of a node's degree, so  $C(z)$  appears as a horizontal line if plotted as a function of  $z$ . The mean path length is proportional to the logarithm of the network size,  $l \approx \log N$  [15], which indicates that it is characterized by the small-world property.

To study the critical behavior of the model we consider the magnetization  $M$ , the susceptibility  $\chi$  and the Binder's fourth-order cumulant, which are defined by

$$M_N(q) = \left[ \left\langle \left| \frac{1}{N} \sum_{i=1}^N \sigma_i \right| \right\rangle_t \right]_s, \quad (2)$$

$$\chi_N(q) = N[\langle m^2 \rangle_t]_s - \langle m \rangle_t^2, \quad (3)$$

$$U_N(q) = 1 - \frac{\langle m^4 \rangle_t]_s}{3\langle m^2 \rangle_t]_s}, \quad (4)$$

where  $N$  is the number of vertices of the random graph with fixed  $z$ ,  $\langle \dots \rangle_t$  denotes time averages taken in the stationary regime, and  $\langle \dots \rangle_s$  stands for sample averages (20 samples).

These quantities are functions of the noise parameter  $q$  and, in the critical region, obey the following finite-size scaling relations

$$M = N^{-\beta/\nu} f_m(x)[1 + \dots], \quad (5)$$

$$\chi = N^{\gamma/\nu} f_\chi(x)[1 + \dots], \quad (6)$$

$$\frac{dU}{dq} = N^{1/\nu} f_U(x)[1 + \dots], \quad (7)$$

the brackets  $[1 + \dots]$  indicate corrections-to-scaling terms,  $\nu$ ,  $\beta$  and  $\gamma$  are the usual critical exponents,  $f_i(x)$  are the finite size scaling functions with

$$x = (q - q_c)N^{1/\nu} \quad (8)$$

being the scaling variable. Therefore, from the size dependence of  $M_N$  and  $\chi$  we obtained the exponents  $\beta/\nu$  and  $\gamma/\nu$ , respectively. The maximum value of susceptibility  $\chi$  also scales as  $N^{\gamma/\nu}$ . Moreover, the value of  $q$  for which  $\chi$  has a maximum,  $q_c^{\chi_{\max}} = q_c(N)$ , is expected to scale with the system size as

$$q_c(N) = q_c + bN^{-1/\nu}, \quad (9)$$

where the constant  $b$  is close to unity. Therefore, the equations 7 and 9 are used to determine the exponent  $1/\nu$ , as well as to check the values of  $q_c$  obtained from the analysis of the Binder's cumulant (Eq. 4). Finally, we have also examined if the calculated exponents satisfy the hyperscaling hypothesis

$$2\beta/\nu + \gamma/\nu = D_{\text{eff}} \quad (10)$$

in order to get the effective dimensionality,  $D_{\text{eff}}$ , for various values of connectivity  $z$ .

We have performed Monte Carlo simulation on *directed* ER random graphs with various values of connectivity  $z$ . For a given  $z$ , we used systems of size  $N = 250, 500, 1000, 2000, 4000, 8000$  and  $16000$ . We waited 10000 Monte Carlo steps (MCS) to make the system reach the steady state, and the time averages were estimated from the next 10000 MCS. In our simulations, one MCS is accomplished after all the  $N$  spins are updated. For all sets of parameters, we have generated 20 distinct networks, and have simulated 20 independent runs for each distinct network.

### 3 Results and Discussion

In Fig. 1 we show the dependence of the magnetization  $M_N$  and the susceptibility  $\chi$  on the noise parameter, obtained from simulations on *directed* ER random graphs with  $N = 16000$  sites and several values of connectivity  $z$ . In Fig. 1(a) each curve for  $M_N$ , for a given value of  $N$  and  $z$ , suggests that there is a phase transition from an ordered state to a disordered state. The phase transition occurs at a value of the critical noise parameter  $q_c$ , which is an increasing function the connectivity  $z$  of the *directed* ER random graphs. In Fig. 1(b) we show the corresponding behavior of the susceptibility  $\chi$ . The value of  $q$  where  $\chi$  has a maximum is here identified as  $q_c(N)$  (Eq. 9).

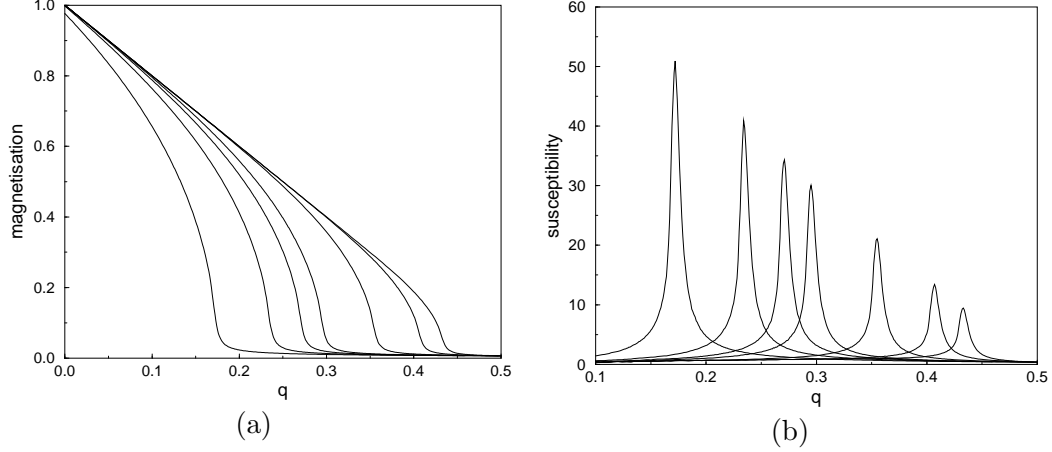


Fig. 1. **(a)** Magnetization and **(b)** susceptibility as a function of the noise parameter  $q$ , for  $N = 16000$  sites. From left to right we have  $z = 4, 6, 8, 10, 20, 50$ , and  $100$ .

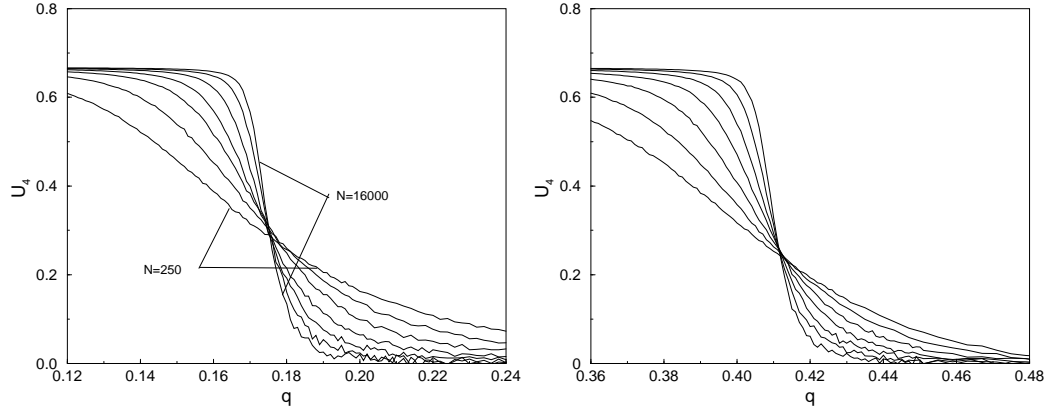


Fig. 2. Binder's fourth-order cumulant as a function of  $q$  for several values of network sizes  $N$  ( $N = 250, 500, 1000, 2000, 4000, 8000$  and  $16000$ ), and for two different values of the connectivity  $z$ :  $z = 4$  (on the left-hand side) and  $z = 50$  (on the right-hand side).

To determine estimates for the critical point  $q_c$ , we calculate the Binder fourth-order magnetization cumulant  $U$  at different values of the noise  $q$  and several network sizes  $N$ . Finite size scaling predicts that for sufficiently large systems, these curves should have a unique intersection point  $U^*$  [27]. The value of  $q$  where this crossing occurs is the value of the critical noise  $q_c$  which is not biased by any assumptions about critical exponents, since by construction, the Binder cumulant presents zero anomalous dimension, therefore it respects the correct critical behavior of the system near  $q_c$  [27,28].

In Fig. 2 we plot the Binder's fourth-order cumulant for different values of  $N$  and two different values of  $z$  ( $z = 4$  and  $z = 50$ ). The critical noise parameter  $q_c$ , for a given value of  $z$ , is estimated as the point where the curves for different system sizes  $N$  intercept each other. As we can noticed, there exists some dependence of the critical noise  $q_c$  with the connectivity  $z$ , i.e., when the

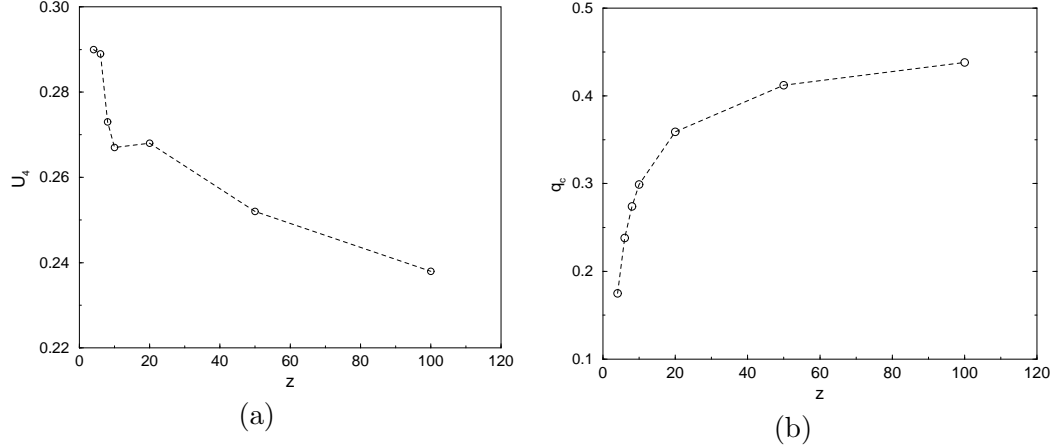


Fig. 3. **(a)** The intersection point  $U^*$  versus the connectivity  $z$ ; **(b)** Phase diagram: the critical values of the noise parameter  $q_c$  as a function of the connectivity  $z$ .

connectivity  $z$  increases, the critical noise also increases: for  $z = 4$ ,  $q_c \approx 0.18$  (left-hand side of accept Fig. 2), and for  $z = 50$ ,  $q_c \approx 0.412$  (right-hand side of Fig. 2). This same procedure is also made for several values of connectivity  $z$ , in this way the Binder's cumulant crossing point  $U^*$  as a function of the connectivity  $z$  could be obtained (Fig. 3(a)), as well as the phase diagram is built, i.e., the dependence of the critical noise  $q_c$  with the node connectivity  $z$ , what is shown in Figure 3(b). Based on the fact that the crossing point of the cumulant (for different system sizes) gives the transition point and the value of the cumulant  $U^*$  at the transition point indicates the universality class of the transition [27]. So, from Fig. 3(a), which shows that the intersection point  $U^*$  of the cumulant decreases when the connectivity  $z$  increases, it can be argued the present model does not fall into the same universality class of the equilibrium Ising model, since  $U^* = 2/3$  well inside the ordered phase and  $U \rightarrow 0$  well within the disordered phase. The Fig 3(b) indicates the increase of the critical noise  $q_c$  with the increase of the node degree  $z$ , and moreover, for higher values of  $z$ , the critical noise  $q_c$  approaches to that one obtained ( $q_c \approx 0.5$ ) from mean-field theory when  $z \rightarrow \infty$  [12]. In addition, according to the mean-field theory [12], in the limit the connectivity  $z$  goes to infinity, the magnetization approaches also to the value 0.5, what one could infer from Fig 1. It is important to emphasize that these results obtained from our Monte Carlo simulations are in a good agreement with a previous work of the majority-vote model with noise on random graphs [12], in which simulations and mean-field analysis were performed to characterize the system transition.

Figure 4(a) and Figure 4(b) show, at  $q = q_c$ , the dependence of the magnetization and the susceptibility with the system size  $N$ , respectively, when different values of the connectivity  $z$  are considered. As we can see, the obtained straight lines, whose slopes correspond to the exponents ratio  $\beta/\nu$  (Fig. 4(a)) and  $\gamma/\nu$  (Fig. 4(b)), confirm the scaling equations, given by Eqs. 5 and

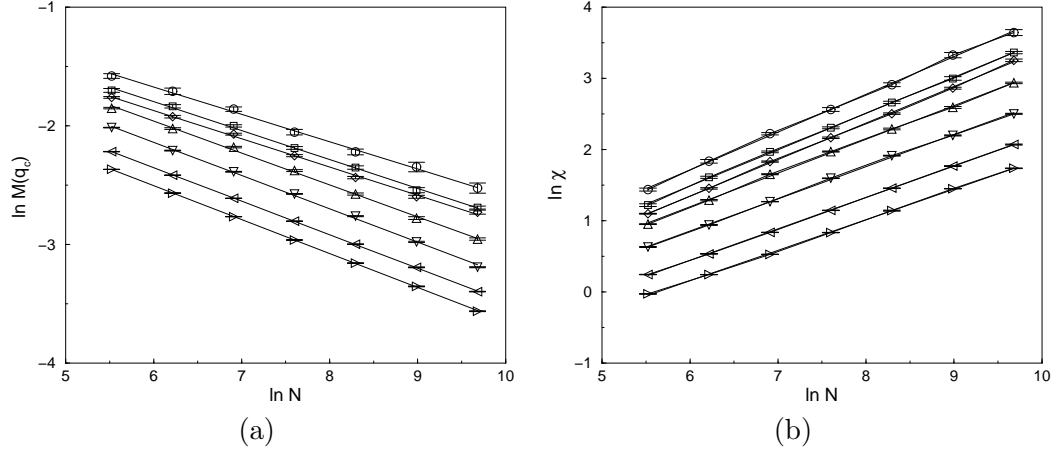


Fig. 4. **(a)**  $\ln M(q_c)$  versus  $\ln N$  and **(b)**  $\ln \chi(q_c)$  versus  $\ln N$ . In both figures, from top to bottom,  $z = 4, 6, 8, 10, 20, 50$  and  $100$ .

6. Moreover, while there is a slight tendency for the exponent  $\beta/\nu$  to increase with  $z$ , the opposite occurs to the exponent  $\gamma/\nu$  that decreases with  $z$ .

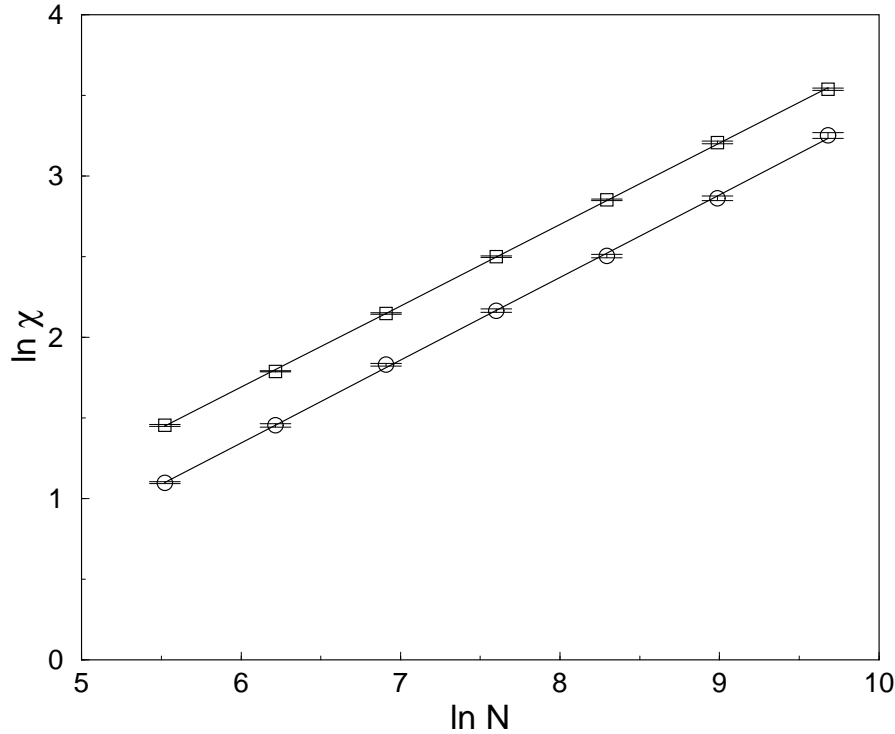


Fig. 5. Log-log plot of the susceptibility at its maximum  $\chi_{\max}$  (squares) and  $q = q_c$  (circles) versus  $N$ , for connectivity  $z = 8$ .

In Fig. 5, we present the dependence, at  $q = q_c$ , of the susceptibility  $\chi$  and of its maximum value  $\chi_{\max}$  with the system size  $N$ . The exponent ratio  $\gamma/\nu$  is obtained from the slopes of the straight lines. For almost all the values of  $z$ , the exponents  $\gamma/\nu$  of the two estimates agree within error bars (see Table 1). As already observed in Fig. 4(b), an increased  $z$  means a slight tendency to



decrease the exponent ratio  $\gamma/\nu$ .

$z$	$q_c$	$\beta/\nu$	$\gamma/\nu^{q_c}$	$\gamma/\nu^{q_c(N)}$	$1/\nu$	$D_{\text{eff}}$
4	0.175(4)	0.230(5)	0.530(6)	0.516(2)	0.545(26)	0.990(7)
6	0.238(3)	0.243(4)	0.509(4)	0.511(2)	0.488(16)	0.995(5)
8	0.274(3)	0.238(4)	0.512(4)	0.504(2)	0.548(14)	0.988(5)
10	0.299(2)	0.268(4)	0.473(5)	0.495(1)	0.487(10)	1.009(6)
20	0.359(2)	0.280(4)	0.451(4)	0.485(2)	0.510(10)	1.011(5)
50	0.412(2)	0.282(3)	0.441(2)	0.466(5)	0.484(11)	1.005(3)
100	0.438(2)	0.286(2)	0.428(3)	0.440(8)	0.520(19)	1.000(3)

Table 1

The critical noise  $q_c$ , and the critical exponents, for *directed* ER random graphs with connectivity  $z$ . Error bars are statistical only.

The Table 1 summarizes the values of  $q_c$ , the three critical exponents  $\beta/\nu$ ,  $\gamma/\nu$ ,  $1/\nu$  and the effective dimensionality of the system. For all values of  $z$ ,  $D_{\text{eff}} = 1$ , which has been obtained from the hyperscaling hypothesis (Eq.10), therefore when  $\beta/\nu$  increases,  $\gamma/\nu$  decreases at  $q_c$ , thus providing  $D_{\text{eff}} = 1$  (along with errors).

It is worth to mention that while our results for the majority-vote model on a *directed* ER random graph are in good agreement with the model on other complex networks, they are different from those found for the majority-vote model and the traditional Ising model on a square lattice [2]. Moreover, the critical exponents and the hyperscaling relation obtained from our simulations corroborate a proposition that the majority-vote models defined on a regular lattice, on small-world networks [9], on Voronoy-Delaunay lattice [10], on Barabási-Albert networks [11,29], and on *undirected* Erdős–Rényi’s random graphs [12], belong to different universality classes.

## 4 Conclusion

Using Monte Carlo simulations, we found a second-order phase transition of the majority-vote model with noise on *directed* ER random graphs. The observed phase transition, which occurs with connectivity  $z > 1$ , was completely characterized through the phase diagram and the critical exponents. Although the obtained exponents are different from those for the same model on other topologies [2,9,10,11,29,30], they suggest that the majority-vote models defined on a regular lattice, on small-world networks, and on Erdős–Rényi’s random graphs, belong to different universality classes. In fact, it was found

that the critical exponents depend on the long-range interactions (short cuts), i.e., they depend on the node degree  $z$ , in such way that results in a larger robustness of the system against the noise: the larger the connectivity  $z$ , the greater the critical noise  $q_c$ . The found values  $U^*$  of the Binder's fourth-order cumulant at the transition point for different values of the connectivity  $z$  were different from those obtained for the isotropic majority-vote model on a regular square lattice and, moreover, for the square Ising model, what corroborates the conjecture that the majority-vote model on complex network does not belong to the same universality class of the equilibrium Ising model. Finally, we should remark that the importance of our results is not only in presenting a set of numbers, but it is in characterizing completely the found phase transition, i.e., to determine the whole set of the critical exponents of the order-disorder phase transition appearing in the system. Moreover, the full set of critical exponents for several values of the connectivity  $z$ , which is really different from the exact values of the Ising model and majority-vote model on a regular lattice, shows clearly the influence of the small-world effects in the majority-vote model, as well as it points out the dependence of the critical exponents with the connectivity  $z$ . Therefore, the well-known effects of the shortest path length in systems with small-world topology on the information propagation are the responsible for making more effective the influence of the neighborhood, which now is not constrained by the geographical distance between the individuals, as observed in regular lattices. Of course, we are aware that random graphs are seldom very good models for the type of networks one finds in nature [17,31]. While they have a low shortest path length, they do not have another important property of most observed networks: clustering. This is obviously not the case in our studied topology, where all vertex pairs are independently connected with the same probability.

## 5 Acknowledgments

F.W.S. Lima acknowledges the Brazilian agency FAPEPI (Teresina-Piauí-Brasil) for its financial support. A.O. Sousa is grateful to the Brazilian Foundation FAPERN for financial support. This work also was supported the system SGI Altix 1350 the computational park CENAPAD.UNICAMP-USP, SP-BRAZIL.

## References

- [1] L. Gray, in *Particle Systems, random Media and Large Deviations*, ed. R. Durrett, American Mathematical Society (Providence – Rhode Island) 1985, p. 149.

- [2] M.J. Oliveira, J. Stat. Phys. **66**, 273 (1992).
- [3] M. A. Santos, S. Teixeira, J. Stat. Phys. **78**, 963 (1995).
- [4] L. Crochik, T. Tomé, Phys. Rev. E **72**, 057103 (2005).
- [5] W. Lenz, Z. Phys. **21**, 613 (1920); E. Ising, Z. Phys. **31**, 253 (1925); M. Hasenbusch, Int. J. Mod. Phys. C **12**, 911 (2001).
- [6] J. J. Binney, N. J. Dowrick, A. J. Fisher, and M. E. J. Newman, *A theory of critical phenomena. An Introduction to the renormalization group*, Clarendon Press (Oxford) 1992.
- [7] G. Grinstein, C. Jayaprakash, and Yu He, Phys. Rev. Lett. **55**, 2527 (1985).
- [8] M.J. de Oliveira, J.F.F. Mendes, and M.A. Santos, J. Phys. A **26**, 2317 (1993); P. Tamayo, F.J. Alexander, and R. Gupta, Phys. Rev. E **50**, 3474 (1995); T. Tomé and J.R. Drugowich de Felício, Phys. Rev. E **53**, 3976 (1996); N.R.S. Ortega, C.F. Pinheiro, T. Tomé and J.R. Drugowich de Felício, Physica A **255**, 189 (1998).
- [9] P.R. Campos, V.M. Oliveira, and F.G.B. Moreira, Phys. Rev. E **67**, 026104 (2003).
- [10] F.W.S. Lima, U.L. Fulco, and R.N. Costa Filho, Phys. Rev. E **71**, 036105 (2005).
- [11] F.W.S. Lima, for Int. J. Mod. Phys. C **17**, 1257.
- [12] L.F.C. Pereira and F.G. Brady Moreira, Phys. Rev. E **71**, 016123 (2005).
- [13] D.J. Watts, S.H. Strogatz, Nature **393**, 440 (1998); M.E.J. Newman and D.J. Watts, Phys. Rev. E **60**, 7332 (1999); M.E.J. Newman and D.J. Watts, Phys. Lett. A **263**, 341 (1999).
- [14] P. Erdős and A. Rényi, Publ. Math. Debrecen **6**, 290 (1959); P. Erdős and A. Rényi, Publ. Math. Inst. Hung. Acad. Sci. **5**, 17 (1960); P. Erdős and A. Rényi, Bull. Inst. Int. Stat. **38**, 343 (1961).
- [15] B. Bollobás, Random Graphs, Academic Press (New York) 1985.
- [16] F. W. S. Lima, J. E. Moreira, J. S. Andrade, Jr., and U. M. S. Costa, Physica A **283**, 100 (2000); F. W. S. Lima, U. M. S. Costa, M. P. Almeida, and J. S. Andrade, Jr., Eur. Phys. J. B **17**, 111 (2000).
- [17] R. Albert and A.L. Barabási, Rev. Mod. Phys. **74**, 47 (2002)
- [18] A. Aleksiejuk, J.A. Holyst and D. Stauffer, Physica A **310**, 269 (2002).
- [19] J.J.F. Mendes and M. A. Santos, Phys. Rev. E **57**, 108 (1998)
- [20] D. Stauffer, J. Artificial Soc. Social Simulations **5**, 1 (2002); D. Stauffer, Conf. 50th Anniversary of the Metropolis Algorithm (2003), in press, cond-mat/0307133; K. Sznajd-Weron and J. Sznajd, Int. J. Mod. Phys. C **11**, 1157 (2000); M.C. Gonzalez, A.O. Sousa and H.J. Herrmann, Int. Journal of

- Modern Physics C **15**, 45 (2004). D. Stauffer, A.O. Sousa, C. Schulze, Journal of Artificial Societies and Social Simulation (2004), A.O. Sousa, Physica A **348**, 701, (2005). Tu Yu-Song, A.O. Sousa, Kong Ling-Jiang and Liu Mu-Ren, Int. J. Mod. Phys. C **17**, (2005).
- [21] G. Defuant, D. Neau, F. Amblard and G. Weisbuch, Adv. Complex Syst. **3**, 87 (2000); G. Weisbuch, G. Defuant, F. Amblard and J.-P. Nadal, Complexity **7**, 55 (2002); G. Defuant, F. Amblard, G. Weisbuch and T. Faure, J. Artificial Soc. Social Simulation **5**, 1 (2002); R. Hegselmann and M. Krause, J. Artificial Soc. Social Simulation **5**, 2 (2002); U. Krause, *Modellierung und Simulation von Dynamiken mit vielen interagierenden Akteuren*, eds. U. Krause and M. Stöckler (Bremen University, 1997), p. 37.
- [22] S. Galam, J. Math. Psychology **30**, 426 (1986); S. Galam, J. Stat. Phys. **61**, 943 (1990); S. Galam, Physica A **285**, 66 (2000); S. Galam, Eur. Phys. J. B **25**, 403 (2002).
- [23] S. Galam, Europhys. Lett. **70**, 705 (2005).
- [24] M.S. de la Lama, J.M. Lopez, H.S. Wio, Europhys. Lett. **72**, 851 (2005); H.S. Wio, M.S. de la Lama and J.M. Lopez, Physica A **371**, 108 (2006).
- [25] Bollobás, *Random Graphs* Academic Press (London) 1985; B. Bollobás, *Modern Graph Theory*, Graduate Texts in Mathematics, Springer (New York) 1998.
- [26] S. Wasserman, K. Faust, B. Bollobás, *Social Networks Analysis*, Cambridge University Press (Cambridge) 1994.
- [27] K. Binder, Z. Phys. B **43**, 119 (1981); K. Binder, in *Finite Size Scaling and Numerical Simulation of Statistical Systems*, edited by V. Privman, World Scientific (Singapore) 1990, 174; D.P. Landau and K. Binder, *A Guide to Monte Carlo Simulations in Statistical Physics*, Cambridge University Press (Cambridge) 2000.
- [28] J.S. Sá Martins and P.M.C. de Oliveira, Braz. J. Phys **34**, 1077 (2004).
- [29] F.W.S. Lima, Commun. Comput. Phys., **2**, 358 (2007).
- [30] Edina M. S. Luz and F.W.S. Lima, for Int. J. Mod. Phys. C.
- [31] S. Boccaletti, V. Latora, Y. Moreno, M. Chavez, D.-U Hwang, Phys. Rep. **424**, 175 (2006).